Dentomaxillofacial Radiology (2007) 36, 211–217

http://dmfr.birjournals.org

RESEARCH

Morphometric analysis of experimentally induced periapical lesions: radiographic *vs* histopathological findings

A De Rossi*[,1], M De Rossi[2], LB Rocha[1], LAB da Silva[3] and MA Rossi[1]

[1]Department of Pathology, Ribeirão Preto School of Medicine, University of São Paulo, Ribeirão Preto, São Paulo, Brazil; [2]Department of Pediatric Dentistry, School of Dentistry of Piracicaba, State University of Campinas, Piracicaba, São Paulo, Brazil; [3]Department of Pediatric Dentistry, Ribeirão Preto School of Dentistry, University of São Paulo, Ribeirão Preto, São Paulo, Brazil

Objectives: To evaluate the accuracy and reliability of conventional (Kodak Ektaspeed Plus™ film) and digitized radiographic images to detect the presence as well to estimate the size, as measured by an image analysis programme, of periapical radiolucencies induced in dog teeth in comparison with the histomorphometric data obtained from the same lesions by conventional and fluorescence microscopy.

Method: After the removal of pulp, the root canals of five premolars from the same animal were left exposed for 7 days after which they were sealed for 60 days. At day 53, three more premolars were opened and left exposed to the oral cavity for 7 days. Intact premolars were used as control. Conventional radiographs were taken at day 0, day 7, day 30, day 45 and day 60. Morphometry in digitized radiographic images and histological sections were compared at day 7 and day 60 after setting the experimental series.

Results: Radiographically, periapical lesions were only detected 30 days after coronal sealing. A progressively increasing radiolucent lesion area was observed at day 45 and day 60. Histopathologically, 7 days after pulp removal dense inflammatory infiltrate and root resorption in the periapical region was observed. At day 7 and day 60, the lesion sizes were similar when evaluated by both conventional and fluorescence microscopy. Lesion size was about 20% larger in digitized radiographs in comparison with histological measurements.

Conclusions: Although image digitization could not improve the detection of the early stages of periapical lesions, it provides a valuable quantitative assessment of extensive periapical lesions. In addition, fluorescence light microscopy enhances the visualization of the apical and periapical structures and seems to be a highly useful tool for histological evaluation, valuable for both qualitative and quantitative studies of periapical disease.

Dentomaxillofacial Radiology (2007) **36,** 211–217. doi: 10.1259/dmfr/93927281

Keywords: radiography, microscopy, fluorescence, periapical disease

Introduction

The introduction of digital imaging techniques in dental practice has created a challenging opportunity to investigate the possibilities of computer-aided image interpretation. In endodontics, to improve the diagnosis of periapical radiolucencies and to make the follow up of extensive periapical lesions more reliable and reproducible, alternative digital image analysis techniques have been proposed.[1–5] However, the reliability of radiographs in detecting and estimating the size of periapical lesions depends on several biological and technical factors that can only be conclusively determined by comparing the radiographic appearance with the histopathological features. Only a few studies employing animal models[1–3] or human biopsies[6–10] have compared the diagnostic and quantifying accuracy of radiographs to the "gold standard" represented by the histology. In addition, in these studies the features of periapical lesions are characterized and their size estimated through linear vertical and horizontal measurements,[8–10] which could not represent the actual dimension of the lesion.

This study evaluates the accuracy and reliability of conventional (Kodak Ektaspeed Plus™ film) and digitized

*Correspondence to: Andiara De Rossi, Department of Pathology, Faculty of Medicine of Ribeirão Preto, University of São Paulo, 14049-900 Ribeirão Preto, São Paulo, Brazil; E-mail: andiaraderossi@bol.com.br
Received 18 January 2006; revised 20 April 2006; accepted 23 May 2006

radiographic images to detect the presence of and estimate the size, as measured by an image analysis programme, of periapical radiolucencies induced in dog teeth in comparison with the histomorphometric data obtained from the same lesions by conventional and fluorescence microscopy.

Materials and methods

All animal procedures performed in this study conformed to protocols reviewed and approved by the Animal Ethical Committee of the University of São Paulo (Protocol #2002.1.121.53.0).

The second, third and fourth mandibular premolars and the second and third maxillary premolars of a healthy mongrel dog (16 months of age, weighing 15 kg) were used (a total of 20 roots). The dog was maintained in a standard cage with water and a standard diet throughout the study. The animal was previously sedated with acepromazine maleate (0.8 mg kg^{-1} intramuscular; Promace; Aveo Co. Inc., Fort Dodge, IA). Surgical procedures were performed under sodium thiopental anaesthesia (30 mg kg^{-1} intravenously; Thionembutal; Abbott Laboratories, São Paulo, SP, Brazil). The dog received lactated Ringer's solution (Lactated Ringer's Inj, USP; Abbott Laboratories, São Paulo, SP, Brazil) during surgery.

Supplemental local infiltration anaesthesia (Xylocaine 2%, 1:100 000 epinephrine; Astra Pharmaceuticals, Westborough, MA) was used at the experimental sites to minimize pain or discomfort. After anaesthesia was achieved, crown access was created on the occlusal surface of three mandibular premolars and two maxillary premolars with spherical carbide burrs (a total of ten roots). After the removal of pulp, the root canals were left exposed for 7 days to allow microbial contamination. The access openings were then sealed with quick-setting zinc oxide—eugenol cement (Pulposan, SS White Artigos Dentários; Rio de Janeiro, RJ, Brazil). At 30 days, 45 days and 60 days after the procedures, conventional radiographs were taken until radiolucent images indicating extensive chronic periapical lesion were obtained. Two more mandibular premolars and one maxillary premolar (a total of six roots) were opened at day 53 as described, left exposed to the oral cavity for 7 days to allow microbial contamination and then sealed with quick-setting zinc oxide—eugenol cement. At this time, the animal was euthanized. This procedure was used to permit the evaluation of periapical lesion formation in initial and advanced stages. One maxillary and one mandibular premolar, both intact, served as controls (a total of four roots) to provide information about the normal anatomical and histological structure of the dog premolar and periapical tissue.

Radiographic analysis

Standardized periapical radiographs were taken using paralleling custom stents at day 0, day 7, day 30, day 45 and day 60. A Heliodent™ (Siemens, Erlangen, Germany) dental radiographic unit was used with standardized exposure settings: 60 kV, 10 mA, 0.4 s and 37 cm focus-film distance. E-speed periapical film (Kodak Ektaspeed™ Plus; Eastman Kodak Company, Rochester, NY) was used. All films were processed on the day of exposure using an automatic film processor (Dent-X film Processor Model 9000; Dent-X, Elmsford, NY).

The conventional radiographs were digitized using an optical scanner (Scanjet 7450C; Hewlett–Packard Development Company, Palo Alto, CA) with a transparency adapter in grayscale mode and with a resolution of 600 dpi. The resulting images were displayed on the screen of a personal computer (Pentium IV CPU at 3.2 GHz, hard disk 120 GB of memory, 1 GB of RAM, 17 inch colour SVGA monitor with 1920 × 1440 pixels of resolution). Evaluation was carried out to determine the presence of a radiolucent area suggestive of a periapical lesion in both conventional and digitized radiographs. Conventional radiographs were examined at the same region on a light viewing box with 2.5 times magnification and with peripheral light excluded. Digitized images were viewed directly at the computer monitor. All morphometric procedures were made by three skilled observers blinded to the treatment groups. The size of each periapical lesion was the mean of the three individual measurements. The morphometric evaluation was performed using the public domain software ImageJ (version 1.33u, National Institute of Health, Washington, DC; available from: http://rsb.info.nih.gov/ij/). The calibration of the programme was carried out for each image using the previously measured real length of the teeth. Delineation was manually performed on the digitized image to exclude tooth and bone intact structure while including the radiolucent areas. The observers manipulated the image magnification, brightness and contrast to threshold the radiolucent periapical lesions and radiopaque alveolar bone.

Histopathological analysis

The material for study was obtained after euthanizing the animal with an anaesthetic overdose. The maxilla and the mandible were removed. The teeth were separated and individually fixed in 2.5% glutaraldehyde in cacodylate buffer with saccharose for 24–48 h at room temperature. The specimens were then washed and demineralized with 4.13% EDTA (ethylenediamenetetraacetic acid) in a microwave oven. The roots were then washed under running water for 24 h, dehydrated in ascending concentrations of ethanol, cleared in xylol and embedded in paraffin. Longitudinal sections 6 μm thick were cut in mesiodistal orientation at the tooth apex level, stained with haematoxylin and eosin and examined, under a light microscope (Leica DMR; Leica Microsystem Wetzlar GmbH, Wetzlar, Germany).

Morphometric analysis was performed using videomicroscopy with the Leica QWin software (Leica Imaging Systems Ltd, Cambridge, UK) in conjunction with the light microscope, videocamera (Leica DC-300F; Leica Microsystems AG, Heerbrugg, Switzerland) and an online computer, as mentioned previously. After the selection of the most appropriate sections (the largest sections simultaneously showing the coronal and apical pulp

through the apical foramen and the connecting periapical tissue), the same three skilled observers masked to the treatment groups made the measurements. Delineation was performed excluding intact tooth and bone structures and including the inflammatory infiltrate areas. If necessary, the observers could manipulate image characteristics of brightness, contrast and magnification to improve the visualization of the inflamed areas of the periapical lesions in tissue sections.

Fluorescence microscopy
Tissue sections stained with haematoxylin and eosin were analysed using the above-mentioned microscope operating in fluorescence mode, using a HBO 100W/2 arc mercury lamp and an I3 filter cube (Leica Microsystem Wetzlar GmbH) with the following characteristics: 450–490 nm bandpass excitation filter, 510 nm dichromatic mirror and 515 nm longpass suppression filter. Using this set-up, the eosin fluoresces, emitting yellowish/greenish light.

Statistical analysis
Data were analysed using the SPSS 10.0 for Windows statistics software (SPSS Inc., Chicago, IL). The Kolmogorov–Smirnov test was used to assess the data distribution. One-way analysis of variance and the Bonferroni test (to correct for multiple comparisons) were used to evaluate the differences between the means of radiographic, conventional and fluorescent microscopic measurements, and between radiographic measurements at 30 days, 45 days and 60 days. $P < 0.05$ was considered statistically significant. Data are presented as mean ± standard error of the mean (SEM).

Results

Radiographic analysis
Conventional radiographs and digitized images revealed the same results concerning the presence or absence of periapical lesions for all examiners. The teeth submitted to pulp removal, leaving the cavities open for 7 days, did not show any radiographic images suggestive of periapical resorption at day 7. Radiographic periapical lesions were first observed at day 30. A progressively increasing area of periapical radiolucent lesions was observed at 45 days and 60 days (Figures 1 and 2). The mean size of the periapical lesions could easily be delineated and measured by the observers in the digitized images, while the conventional radiography did not allow the use of any efficient method to evaluate the dimension of the periapical lesion. There was no statistically significant difference between the mean sizes of the periapical lesions obtained by the three observers.

Histopathological analysis

Control specimens:
Day 0. The intact premolars showed vital pulp tissue and normal periapical region. A large single canal with an apical delta could be seen in the dog premolar. The periodontal ligament was mostly composed of fibroblasts, interspersed with collagen fibres and numerous vascular and neural elements (Figure 1). The same area observed in fluorescence mode revealed the complex architecture of the periodontal ligament, the varying sizes of fibre bundles, the specific spatial alignment of collagen fibres, showing its origin inserted in dental cementum, its fibres running perpendicular to teeth surface inserting in the alveolar bone, many running deep into the bone trabeculae. Cell occupied spaces appear as black dots in the cellular cementum, alveolar bone and among the collagen fibres in the periodontal ligament (Figure 3).

Experimental specimens:
Day 7. Specimens submitted to pulp removal leaving the cavities open for 7 days presented either empty root canals or root canals with remnants of necrotic pulp tissue and debris. The surface of the root apex was corrugated with lacunae indicating initial cementum resorption (Figure 1). The periapical region was capped by a twin layer of inflammatory cells, mainly neutrophils, histiocytes, xanthomatous histiocytes, plasma cells and lymphocytes. Bone surface resorption areas (Howship's lacunae) were evident similar to the cementum surface. Fluorescence microscopy (Figure 3) showed that the lesion consisted of a loose connective tissue. Observation at low magnification showed areas of low brightness. The periodontal ligament was completely destroyed at the bone side. On the other hand, ligament fibres still remained attached to the cementum.
Day 60. Specimens submitted to pulp removal, leaving the cavities open for 7 days and then sealing for 60 days, presented root canals usually containing remnants of necrotic pulp tissue and debris. The surface of the root apex was frequently corrugated with large lacunae indicating advanced cementum resorption. The periapical region was capped by extensive and dense chronic inflammatory infiltrate composed of histiocytes, xanthomatous histiocytes, plasma cells, lymphocytes and few neutrophils. Bone surface resorption areas were more evident (Figure 1). These periapical lesions could be clearly detected and delineated with fluorescence microscopy (Figure 3). The periodontal ligament fibres became shorter as the lesion evolved from day 7 to day 60, but they were absent only from the teeth surface where the cementum had started to be resorbed. Only intact fibres showed strong green fluorescence.

Radiographic vs *conventional and fluorescence microscopy morphometry:* Figure 2 shows the comparison of the morphometric evaluation between digitized radiographic image, conventional and fluorescence microscopy. At day 7 and day 60, there were statistically significant differences between the mean size of the periapical lesions comparing radiographic and conventional and fluorescence microscopy ($P < 0.001$). Lesion size was about 20% larger in digitized radiographs than in histological sections. There was no significant difference in the rate of histological lesion size between conventional and fluorescence microscopy measurements. However, the

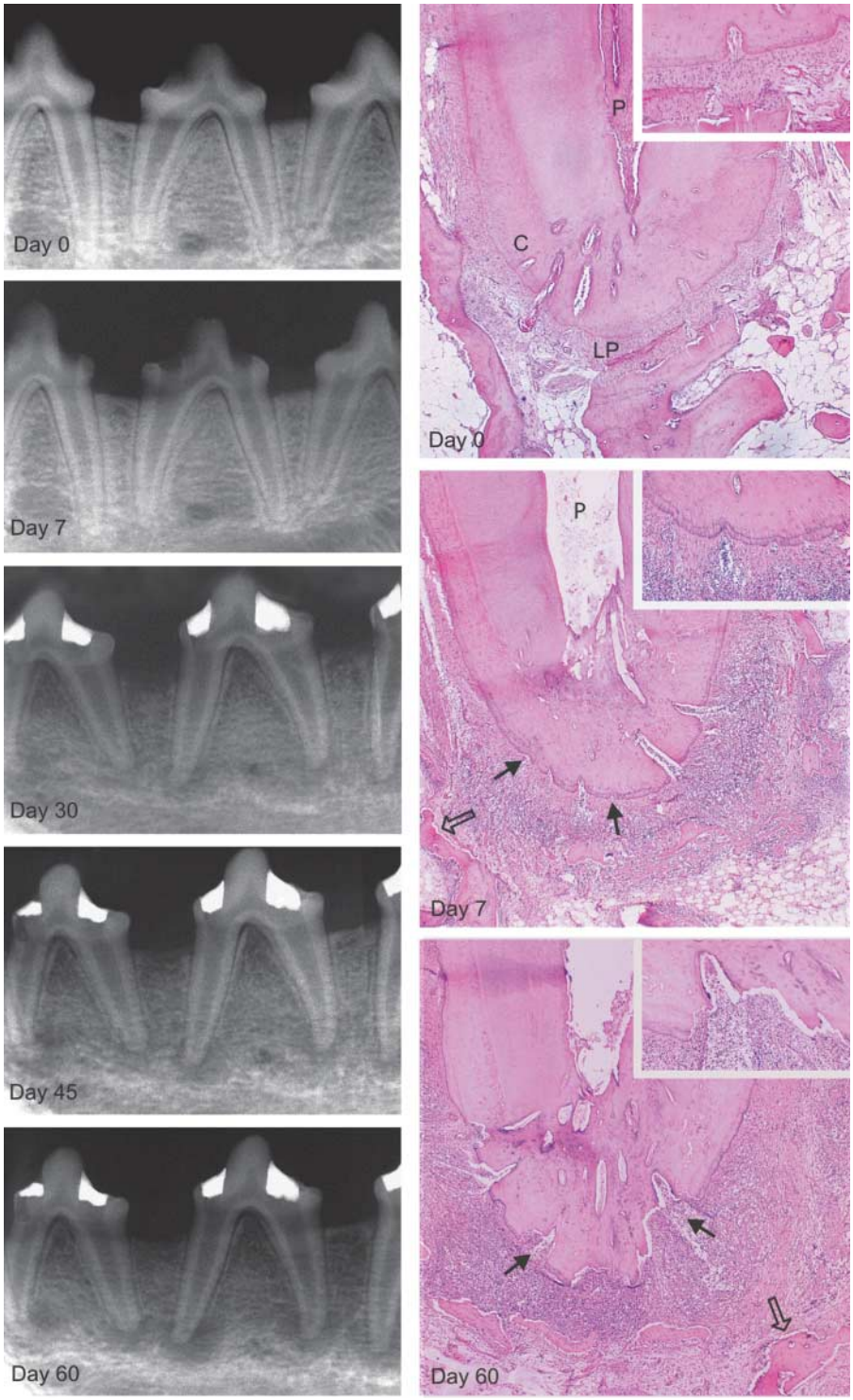

Figure 1 Radiographic digitized images and representative light microscopic features of the periapical region from intact control tooth (day 0), tooth submitted to pulp removal leaving the cavity open for 7 days (day 7) and teeth with pulp removal leaving the cavity open for 7 days and then sealing (day 30, day 45 and day 60). At day 0, normal periapical radiographic appearance is in accordance with normal histological features showing integrity of pulp tissue (P), cementum (C) and periodontal ligament (LP). At day 7, no radiographic changes can be detected in the periapical region contrasting with necrotic pulp (P) and periapical inflammatory infiltrate. The radiographic images at day 30, day 45 and day 60 clearly show progressively increasing areas of periapical radiolucency. Histologically, at day 60, marked periapical lesion characterized by striking cementum (arrows) and bone (open arrows) resorptions associated with massive chronic inflammatory infiltrate can be seen. (Haematoxylin and eosin; magnification of all panels, × 78; inset, × 150.)

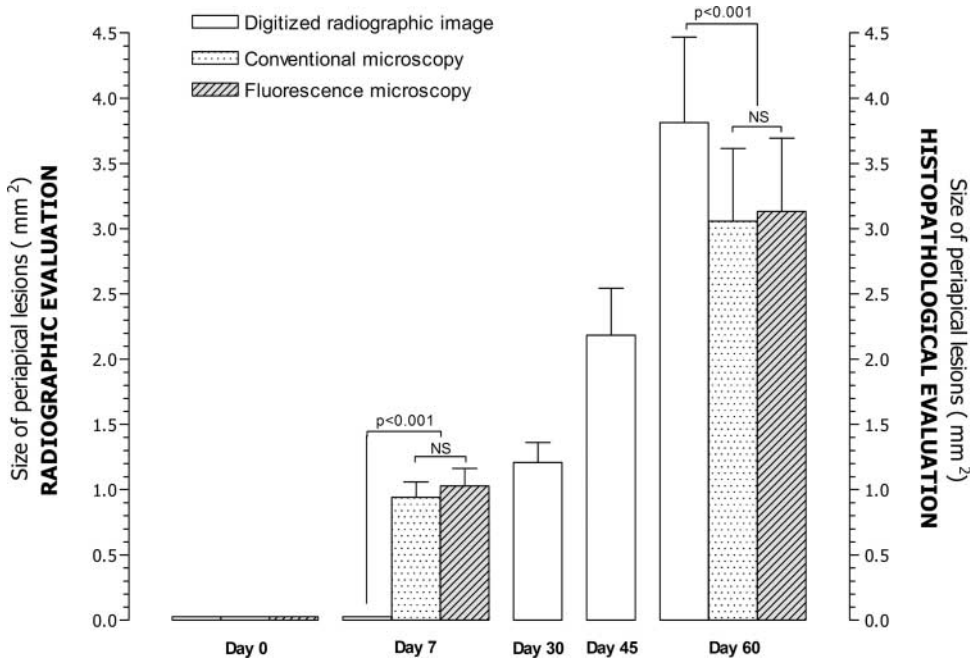

Figure 2 Radiographic (left *y*-axis) and conventional and fluorescence microscopy morphometric analyses (right *y*-axis; rates ± SEM) of the periapical lesion size (in mm^2) from intact control teeth (day 0), teeth submitted to pulp removal leaving the cavities open for 7 days (day 7) and teeth submitted to pulp removal, leaving the cavities open for a week and then sealing at day 30, day 45 and day 60. NS, not significant

fluorescence microscopy enhanced the visualization of the periapical lesion during the measurement procedures.

Discussion

The radiographic and histopathological findings clearly show that the procedure used in the present study can consistently induce periapical lesions in dog teeth. This methodology, similar to that used by others,[4,5,11] confirms the effectiveness of the model for experimental induction of periapical lesions. The benefit of using the dog model in our study was primarily that 20 roots (three mandibular premolars and two maxillary premolars per quadrant) were available for endodontic treatment. This way, an adequate number of observations in the same animal predicted the influence of response variability between animals. Conventional radiographic techniques, such as bisecting angle and paralleling, can also be easily used in the dog model, which is often impossible with smaller animals. The dog has predominantly been used in endodontic research to evaluate the biocompatibility of newly developed materials and the healing process of periapical lesions.[1,4,5,11]

Early detection of periapical radiolucencies associated with pulp necrosis is of paramount importance in endodontic practice as it affects the treatment planning.[5,11] The comparison of our radiographic and histopathological findings discloses the poor reliability of both conventional and digitized radiographs in the diagnosis of early stages of periapical lesions. The histopathological changes present at 7 days could not be detected radiographically. Previous studies have demonstrated the difficulties associated with conventional radiographic evaluation to recognize the presence of early apical root resorption,[7,12] particularly when clinical examination is based on a single radiograph.[10]

Several biological and technical factors can make the detection of apical root resorption on radiographs difficult. The biological factors include the size and location of the resorptive defects, anatomical variations of the jaw and teeth, and their mineral content. Technical factors include the type and number of radiographs, the angle of incidence of the X-ray beam, exposure time, film sensitivity and processing procedures.[13–15] It has been shown that examination of several radiographs taken with different angulations and comparison with previous radiographs enhances the chances of visualization of root resorption,[13,14] but in a clinical situation the number of radiographs taken is usually limited. In the present study, only one radiograph was taken and evaluated at each experimental period. However, the use of a custom stent especially adjusted for each quadrant allowed the standardization of the location and angle of incidence of the X-ray beam during the different periods of the experiment.

In the present study, at day 60, when the lesions were advanced, their mean size in digitized radiographs was larger than that measured microscopically. Previously, the mean sizes of periapical lesions as evaluated by conventional radiograph or CT were shown to be non-different.[9] Contrastingly, other studies have shown a larger preoperative macroscopic size of the periapical lesions in comparison with the size obtained from conventional and digital radiographs.[8,10] These latter results, however, cannot be compared with ours because the periapical lesion sizes were assessed both macroscopically and radiographically measuring the linear vertical and

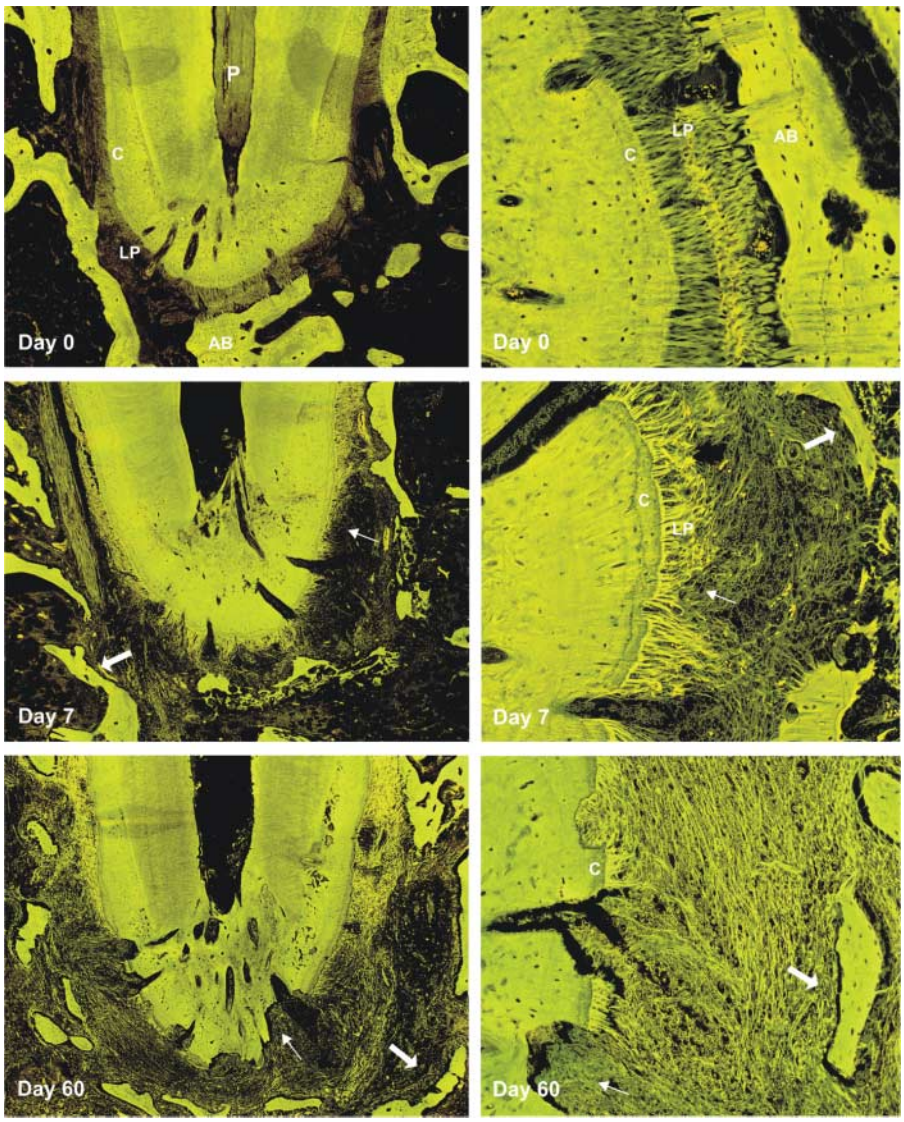

Figure 3 Representative autofluorescent microscopic images of the periapical region from intact control tooth (day 0), tooth submitted to pulp removal leaving the cavities open for 7 days (day 7) and teeth submitted to pulp removal leaving the cavities open for a week and then sealing (day 60). This technique properly demonstrates the integrity of the periapical region in control tooth, contrasting with the periapical region with incipient lesion at day 7 and striking lesion at day 60. At day 0, normal periapical radiographic appearance is in accordance with normal histological features showing integrity of pulp tissue (P), cementum (C) and periodontal ligament (LP). At day 7, the periapical region presented necrotic pulp (P) and periapical inflammatory infiltrate. At day 60, marked periapical lesion characterized by striking cementum (arrows) and bone (open arrows) resorptions associated with massive chronic inflammatory infiltrate can be seen. (Haematoxylin and eosin; magnification $\times 65$; $\times 255$.)

horizontal dimensions. Importantly, the sizes of the periapical radiographic lesions in the present study can be considered actual since for each image the programme was calibrated using the previously measured real length of the teeth. Thus, possible interferences of the radiographic technique due to the angle of incidence of the X-ray beam that could distort the lesions size were strikingly minimized. In addition, the difference between the size of radiographic and histological lesions was about 20%, very close to the usual soft tissue shrinkage caused by formalin fixation and paraffin embedding.[16]

Technological developments, such as digital radiography or CT, have been shown to be helpful in radiographic management of extensive periapical lesions,[2,3] significantly improving image visualization and allowing tridimensional reconstruction. The routine use of CT, however, is too expensive and releases high-dose radiation, although dose reduction methods have been proposed.[17] Although the digitalization of conventional dental radiographs using current high-grade scanners or digital cameras does not produce images of better diagnostic quality,[18] digitization of standardized radiographs still appears to be an easier inexpensive procedure that can be useful in endodontic practice and research, allowing enhanced image visualization, long-term storage, quantitative evaluation and reproducible follow up. There seems to be an agreement on the fact that digitizing the conventional radiographs provides the opportunity to

utilize the image processing tools that may improve subjective image quality.[19,20]

The haematoxylin and eosin-stained sections examined with epi-illumination improved the visualization of apical and periapical structures of dog teeth, particularly the disarray of collagen fibres in the periodontal ligament and the extent of root and bone resorption in both initial and late extensive periapical lesions. This distinct feature of the fluorescent image generated a highly contrasted view of the specific spatial fibre arrangement and structural details. This methodology is possible as eosin is a xanthene dye obtained by halogenization of fluorescein.[21] Although the absorption and emission maxima of eosin in alcoholic solution are 527 nm and 550 nm,[21] with both peaks lying in the green light range, we achieved a highly satisfactory emission illuminating the tissue sections with blue light (450–490 nm) using a commercially available fluorescein filter. For this reason, it was possible to analyse haematoxylin and eosin-stained sections with two different microscopic techniques, attaining two distinctive insights on the morphological aspects of normal and pathological tissues. At 60 days, observation at low magnification showed bone and cementum resorbed areas with low brightness. Only intact fibres showed strong green fluorescence. Despite the fact that conventional and fluorescence microscopic measurements were not significantly different, the delineation and visualization of the periapical lesion extent could more easily be done under fluorescence microscopy.

In conclusion, although image digitization could not improve the detection of the early stages of periapical lesions, it provides valuable quantitative assessment of extensive periapical lesions. In addition, fluorescence light microscopy enhanced the visualization of the apical and periapical structures and seems to be a highly useful tool for histological evaluation and valuable for both qualitative and quantitative studies of periapical disease.

Acknowledgments

This study was supported by grants from Fundação de Amparo à Pesquisa do Estado de São Paulo, São Paulo, Brazil (03/13940-0, 04/03419-3 and 04/14578-5). Professor Rossi is a Senior Investigator of the Conselho Nacional de Desenvolvimento Científico e Tecnológico. The authors thank the expert technical assistance of Maria Elena Riul.

References

1. Delano EO, Tyndall D, Ludlow JB, Trope M, Lost C. Quantitative radiographic follow-up of apical surgery: a radiometric and histologic correlation. *J Endod* 1998; **24:** 420–426.
2. Cotti E, Vargiu P, Dettori C, Mallarini G. Computerized tomography in the management and follow-up of extensive periapical lesion. *Endod Dent Traumatol* 1999; **15:** 186–189.
3. Balto K, Muller R, Carrington DC, Dobeck J, Stashenko P. Quantification of periapical bone destruction in mice by micro-computed tomography. *J Dent Res* 2000; **79:** 35–40.
4. Grecca FS, Leonardo MR, Silva LAB, Tanomaru Filho M, Borges MA. Radiographic evaluation of periradicular repair after endodontic treatment of dog's teeth with induced periradicular periodontitis. *J Endod* 2001; **27:** 610–612.
5. De Rossi A, Silva LAB, Leonardo MR, Rocha LB, Rossi MA. Effect of rotary or manual instrumentation, with or without calcium hydroxide/1% chlorhexidine intracanal dressing, on the healing of experimentally induced chronic periapical lesions. *Oral Surg Oral Med Oral Pathol Oral Radiol Endod* 2005; **99:** 628–636.
6. Brynolf I. A histological and roentgenological study of the periapical region of human upper incisors. *Odontol Revy* 1967; **18(Suppl 11):** 1–176.
7. Laux M, Abbott PV, Pajarola G, Nair PN. Apical inflammatory root resorption: a correlative radiographic and histological assessment. *Int Endod J* 2000; **33:** 483–493.
8. Farman AG, Avant SL, Scarfe WC, Farman TT, Green DB. *In vivo* comparison of Visualix-2 and Ektaspeed Plus in the assessment of periradicular lesion dimensions. *Oral Surg Oral Med Oral Pathol Oral Radiol Endod* 1998; **85:** 203–209.
9. Marmary Y, Koter T, Heling I. The effect of periapical rarefying osteits on cortical and cancellous bone. A study comparing conventional radiographs with computed tomography. *Dentomaxillofac Radiol* 1999; **28:** 267–271.
10. Scarfe WC, Czerniejewski VJ, Farman AG, Avant SL, Molteni R. *In vivo* accuracy and reliability of color-coded image enhancements for the assessment of periradicular lesion dimensions. *Oral Surg Oral Med Oral Pathol Oral Radiol Endod* 1999; **88:** 603–611.
11. Katebzadeh N, Sigurdsson A, Trope M. Radiographic evaluation of periapical healing after obturation of infected root canals: an *in vivo* study. *Int Endod J* 2000; **33:** 60–66.
12. Pitt Ford TR. The radiographic detection of periapical lesions in dogs. *Oral Surg Oral Med Oral Pathol Oral Radiol Endod* 1984; **57:** 662–667.
13. Bender IB. Factors influencing the radiographic appearance of bone lesions. *J Endod* 1982; **8:** 161–170.
14. Andreasen FM, Sewerin I, Mandel U, Andreasen JO. Radiographic assessment of simulated root resorption cavities. *Endod Dent Traumatol* 1987; **3:** 21–27.
15. Goldberg F, De Silvio A, Dreyer C. Radiographic assessment of simulated external root resorption cavities in maxillary incisors. *Endod Dent Traumatol* 1998; **14:** 133–136.
16. Zarins CK, Zatina MA, Glagov S. Correlation of post mortem angiography with pathologic anatomy: quantitation of atherosclerotic lesions. In: Bond MG, (editor). *Clinical diagnosis of atherosclerosis; quantitative methods of evaluation*. New York, NY: Springer, 1986, pp 283–306.
17. Dula K, Mini R, van der Stelt PF, Lambrecht JT, Schneeberger P, Buser D. Hypothetical mortality risk associated with spiral computed tomography of the maxilla and mandible. *Eur J Oral Sci* 1996; **104:** 503–510.
18. Goga R, Chandler NP, Love RM. Clarity and diagnostic quality of digitized conventional intraoral radiographs. *Dentomaxillofac Radiol* 2004; **33:** 103–107.
19. Lehmann TM, Troeltsch E, Spitzer K. Image processing and enhancement provided by commercial dental software programs. *Dentomaxillofac Radiol* 2002; **31:** 264–272.
20. Parissis N, Kondylidou-Sidira A, Tsirlis A, Patias P. Conventional radiographs *vs* digitized radiographs: image quality assessment. *Dentomaxillofac Radiol* 2005; **34:** 353–356.
21. Fleming GR, Knight AWE, Morris JM, Morrison RJS, Robinson GW. Pico second fluorescence studies of xantene dyes. *J Am Chem Soc* 1977; **99:** 4306–4311.